Electronic Supplementary Material (ESI) for Materials Horizons.

Supporting Information

Soft lamellar solid foams from ice-templating of self-assembled lipid hydrogels: organization drives the mechanical properties

Niki Baccile,[a*] Ghazi Ben Messaoud,[a,†] Thomas Zinn,[b] Francisco Fernandes[a,*]

[a] Sorbonne Université, Centre National de la Recherche Scientifique, Laboratoire de Chimie de la Matière Condensée de Paris, LCMCP, F-75005 Paris, France

[†] Current address: DWI- Leibniz Institute for Interactive Materials, Forckenbeckstrasse 50, 52056 Aachen, Germany

[b] ESRF - The European Synchrotron, 71 Avenue des Martyrs, 38043 Grenoble, France

Materials and Methods

Products. Acidic deacetylated C18:0 sophorolipids (SLC18:0) and acidic deacetylated C18:0 glucolipids (GC18:0) have been used from previously existing batch samples, the preparation and characterization of which is published elsewhere.[1,2] Acid (HCl 37%) and base (NaOH) are purchased at Aldrich. MilliQ-quality water has been employed throughout the experimental process. 18:1 Liss Rhod PE (Liss) (M_w= 1301.7 g.mol^{-1}, λ_{abs}= 560 nm, λ_{em}= 583 nm), 1,2-dioleoyl-sn-glycero-3-phosphoethanolamine-N-(lissamine rhodamine B sulfonyl) (ammonium salt), is purchased by Avanti® Polar, Inc.

Self-assembly and preparation of hydrogels. GC18:0 and SLC18:0 are glycolipids respectively constituted by a β-D-glucose and sophorose (D-glucose β(1,2)) headgroup linked to stearic acid via a glyosidic bond located on the C17 carbon of stearic acid (Figure 1). Their self-assembly properties to form bilayers (GC18:0) and twisted flat ribbons (SLC18:0) were reported by us.[1,2,3] Briefly, the selected molecule is introduced in water at the indicated concentration (please refer to the main text for the exact values), and to promote solubility, the pH is raised at values between 10 and 11, at which both compounds mainly form micelles. pH is then reduced to about pH 6.2 ± 0.3 according to the procedure published elsewhere.[4,5] Fibrillar SLC18:0 gels are nicely obtained by a controlled (< 50 μL/h) acidification using 0.5 M or 1 M HCl solutions.[5] Slow acidification is crucial to obtain a gel, as explained in ref. 5. Acidification of lamellar hydrogels can also be carried out by hand but intercalating sonication and vigorous vortexing during each acid addition below pH 8, otherwise local lamellar aggregates form. An alternative, highly reproducible, procedure to prepare GC18:0 lamellar gels was detailed in ref. 4 and consists in simply dispersing the smaple in water, followed by sonication and adjustment of pH to 6.2 and ionic strength to about 100 mM. Sonication (10-15 min) and gentle heating at 70°C during less than 5 min followed by cooling provides a stable gel within less than 2 h. For the GC18:0 system, the method of reaching a final pH of 6.2 is not important, as long as solution is homogeneous and the total ionic strength below 100 mM. Both hydrogels can be processed as such after their preparation.

Solid foams by freeze-casting. The unidirectional freeze-casting setup is home-built according to the literature.[6,7] The setup consists in a liquid nitrogen Dewar, a 40 cm copper bar (Ø¼1.5 cm), a

heating element and a polypropylene tube partially inserted in the hot end of the copper bar to hold the sample prior to freezing. A silicon mold (1 cm x 1 cm x 1 cm) sitting on top of the copper bar was occasionally used for those experiments requiring longitudinal and transverse analysis of the mechanical properties, as clearly indicated in the legends of the corresponding figures in the main text. *Note: The direction of freeze-casting, that is of the ice-growing front, is identified as the Z-axis throughout the paper. Nomenclatures ∥Z and ⊥Z respectively refer to longitudinal and transversal directions with respect to the ice-growing front.*

The assembly was carried out in such a manner that half of the copper bar plunges into liquid N_2 to create a heat sink. The temperature of the opposed extremity of the copper was controlled by the simultaneous action of the heat sink and the heating element. The heating element was controlled by a dedicated PID thermocontroller able to modulate the cooling rate between 1°C.min^{-1} and 10°C.min^{-1}. A temperature sensor (K thermocouple) is located at the bottom of the cell, close to the tip of the copper bar. In a typical experiment, 2 mL of the selected self-assembled glycolipid sample (in solution or hydrogel state) is poured inside the polypropylene tube, in direct contact with the copper surface. After a 5 min equilibration time at 20°C, the sample is cooled down to -60°C, removed from the setup and placed at -20°C before freeze drying. Ice sublimation is systematically conducted on all freeze-cast samples in a Christ Alpha 2-4 LD freeze dryer. The temperature of the freeze dryer condenser is kept below -60°C and the internal pressure stabilized within few minutes to approximately 5 x 10^{-5} bar. The freeze drying process is left to proceed for 24 h, allowing for the recovery of a dried lightweight, macroporous, soft solid, which will be referred to as a solid foam throughout this work.

Small Angle X-ray Scattering (SAXS): SAXS experiments have been performed on the ID02 beamline at the ESRF synchrotron facility (Grenoble, France). The experiments have been done at 17.0 keV and two sample-to-detector distances were used: 2 m and 8 m. Calibration of the q-range is done using silver behenate as classical standard (d_{ref} = 58.38 Å). The signal of the CCD camera, used to record the data, is normalized and integrated azimuthally.[8] to obtain the typical one-dimensional scattering profile I(q) i.e. scattered intensity versu scattering vector q, where q is given by $4\pi/\lambda \sin(\theta)$ with the scattering angle 2θ. The scattered intensity I(q) is given in the dimensionless units of sr^{-1}. I(q) data are presented as such and have not been corrected for the empty and water cell has been performed. Typical acquisition times were in the order of 100 ms,

which we considered enough to obtain a good signal-to-noise profile, with no beam damage observed. One spectrum per temperature value or per time is recorded.

The typical freeze-casting experiment has been adapted to the beamline via a home-made freeze-casting device, which exposes a 2 mm flat cell to beam, whereas the cell is supported by a plastic holder containing two face-to-face Kapton© windows. The image and scheme of the device are shown in Figure S 3a,b. The heating element is controlled by a dedicated PID thermocontroller able to modulate the cooling rate between 1°C.min^{-1} and 10°C.min^{-1}. Temperature is hence controlled between +20°C and -60°C. The SAXS patterns are recorded at a step of 5°C in the entire temperature range at different positions in the cell: for each temperature, the signal is collected at five positions (Z-axis) simultaneously, namely, 100 μm (the closest to the bar), 500 μm, 900 μm, 1300 μm, 1700 μm from the top of the copper bar (Figure S 3b). Movement of the stage along Z is controlled by an automated stage available at the beamline. Both the acquisition time and the stage displacement are fast enough (~ second, including signal acquisition and displacement for the five positions) with respect to the cooling rate, which is 0.17 °C.s^{-1} for the fastest rate. In view of these considerations, one can consider that the measurement can be considered instantaneous (the sample is in the same physical state for all positions at a given measurement time) for all positions.

Scanning Electron Microscopy with Field Emission Gun (SEM-FEG): SEM-FEG experiments have been recorded on a Hitachi SU-70. The images were taken in secondary electron mode with an accelerating voltage at 1 kV, 5 kV or 10 kV. Prior to analysis, the materials were coated with a thin layer of gold by sputter deposition. Both the $\parallel Z$ and $\perp Z$ sections of the samples were systematically observed. SEM images have been treated using the software Image-J,[9] and in particular the local roughness analysis has been done using the roughness calculation plugin, freely available and implemented for ImageJ. The local roughness analysis is measured on the whole surface and it gives roughness values according to the ISO 4287/2000 standard. We present the root mean square roughness, $R_{RMS} = \sqrt{\frac{1}{n}\sum_{i=1}^{n} y_i^2}$, where the roughness profile contains n equally spaced points along the trace, and where y_i is the vertical distance from the mean line to the ith data point. Height is assumed to be positive in the up direction, away from the bulk material.

X-Ray Diffraction (XRD): XRD experiments have been recorded on a Bruker D8 Advance using a classical Bragg Brentano θ-2θ configuration. A copper K_α anticathode with a wavelength λ= 0.154 nm is used. A 1D LynxEye detector is used. We have employed a 0.05° step and 0.5 s/step as acquisition parameters.

Fourier Transform InfraRed spectroscopy (FTIR): FTIR experiments have been done in the ATR mode using a Perkin Elmer Spectrum 400 instrument.

Rheology: Viscoelastic measurements were carried out using an Anton Paar MCR 302 rheometer equipped with parallel titanium or stainless steel sandblasted plates (diameter 25 mm). All experiments were conducted at 25 °C and the temperature was controlled by the stainless steel lower plate, which is the surface of the Peltier system. During experiments, the measuring geometry was covered with a humidity chamber to minimize water evaporation. To characterize the hydrogels, strain sweep experiments were first conducted by changing the shear strain (γ) from 0.001% to 100% to determine the linear viscoelastic regime (LVR). After loading a new sample, values between γ = 0.02 – 0.05 % within the LVR were used in the subsequent angular frequency sweep from ω = 100 and 0.01 $rad.s^{-1}$.

Mechanical analysis: the mechanical properties of the freeze-cast matrices were carried out on an Anton Paar MCR 302 rheometer equipped with a force transducer of 50 N and a plate-plate (25 mm) geometry. The freeze-cast foams obtained from SLC18:0 being friable, the uniaxial compression experiments were conducted only on GC18:0 samples prepared at a freezing rate of $5°C.min^{-1}$. The foams were compressed along the Z-axis from 10 mm to 0.2 mm with a linear compression speed of 5 $\mu m.s^{-1}$. The gap (l) and the normal force (F) being imposed were measured simultaneously at the upper plate. The force-displacement responses were re-plotted in terms of stress (σ) and strain (ε), with $\varepsilon(\%) = \frac{l_0 - l}{l_0} * 100$, where l_0 (m) is the original height of the foam and l (m) is the current height during compression; $\sigma(kPa) = \frac{F}{A*1000}$, where A (m^2) is the cross-sectional area of the foams.

Confocal Laser Scanning Microscopy (CLSM): CLSM was performed with a LeicaSP8 Tandem Confocal system. Samples were excited with the dye specific wavelength (561 nm) and the emission was detected between 580 and 620 nm using a photomultiplier tube (PMT) detector. CLSM images were analyzed using FIJI[9] and 3D construction and projection from Z-stacks was performed using the 3D visualization module of the Leica Application Suite X (LAS X) software. The GC18:0 lamellar solid foam for the CLSM experiments was prepared as follows: a volume of 4 μL of an ethanolic solution of 18:1 Liss Rhod PE (C= 53 mg/mL) was added to 1.5 mL of the GC18:0 hydrogel ($C_{G\text{-}C18:0}$= 2.5 wt%, pH 6) to reach an approximate molar ratio of G-C18:0/Liss of 500. Liss is a water insoluble, rhodamine-containing, lipid and it is largely used to mark lipid bilayers. It is generally considered not to interfere with the bilayer assembly at Lipid/Liss ratio above 200. We did not observe any variation in the gel physical aspect after addition of Liss. The gel was freeze-cast at a rate of 5°C/min in a from 20°C to -60°C, freeze-dried et analyzed. The foams were analyzed both $\perp Z$ and $\parallel Z$, respectively the orthogonal and longitudinal planes with respect to the ice-growth direction (*Z*-axis).

Orientation analysis of the foams structures was performed $\parallel Z$ on sequential *Z* planes obtained from CLSM volumetric data (videos 1 and 4). Fourier components were computed and binned between $-90° < \varphi < 90°$ using the directionality tool on FIJI software.

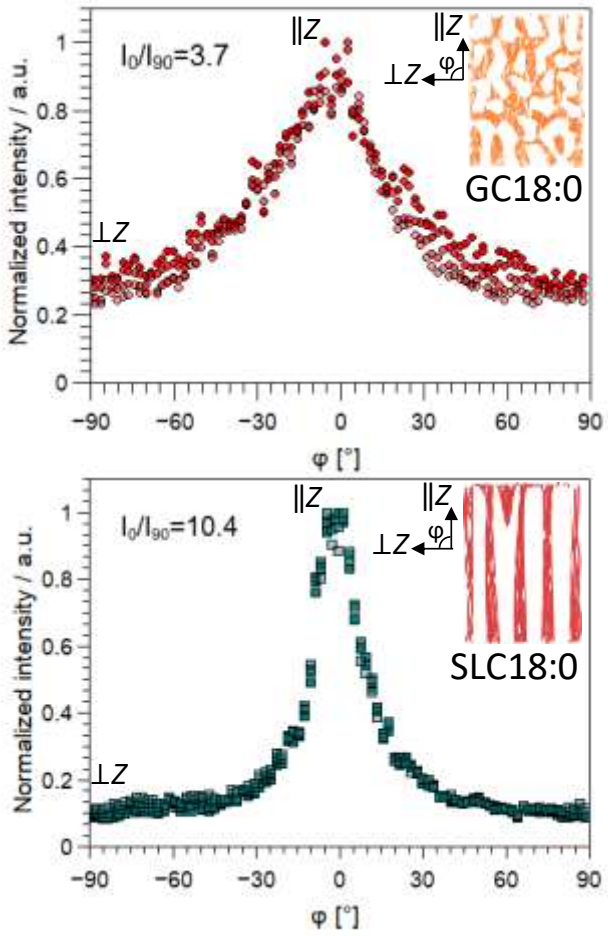

Figure S 1 – Orientational distribution of the intensity measured on four sequential planes obtained form volumetric CSLM data presented on Video 1 and Video 4, respectively for lamellar GC18:0 and fibrillar SLC18:0 solid foams.

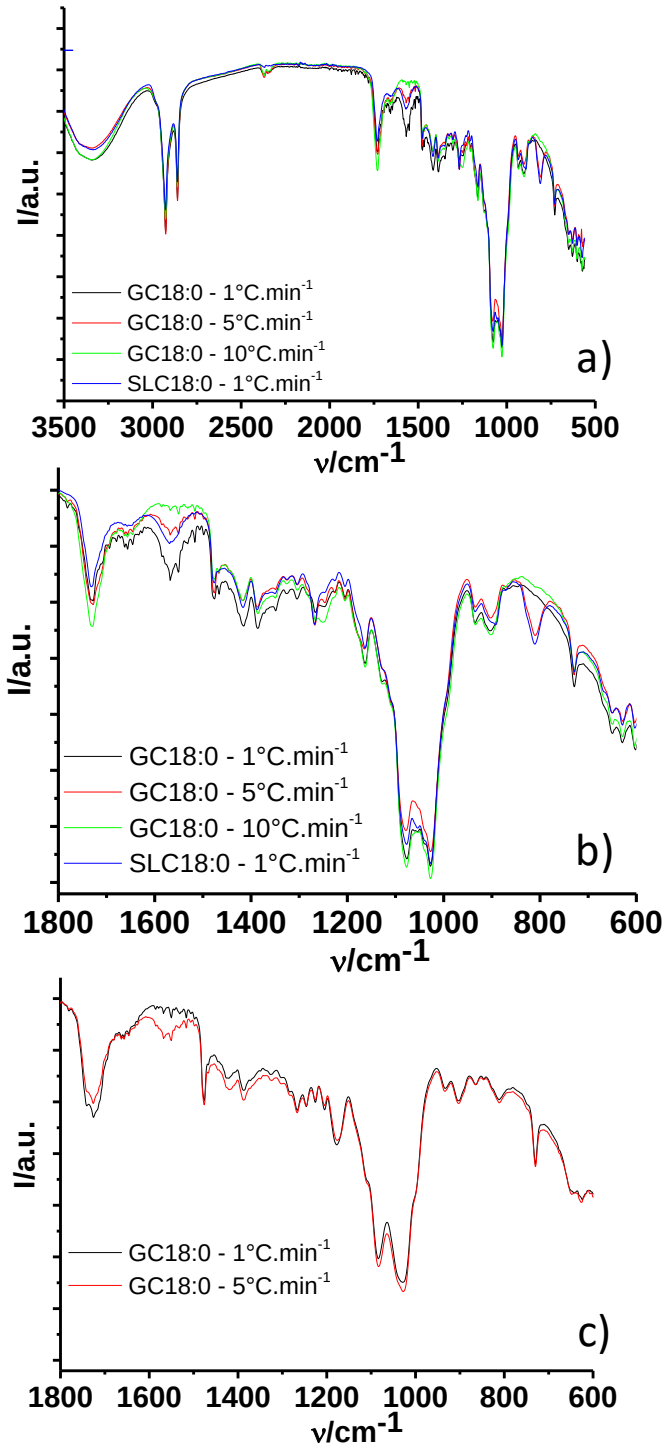

Figure S 2 – a) FT-IR experiments performed on SLC18:0 and GC18:0 solid foams freeze-cast at various freezing rates. b-c) Highlight of the 1800 – 600 cm^{-1} region of the FT-IR spctrum and zoom on the GC18:0 sample alone (c)

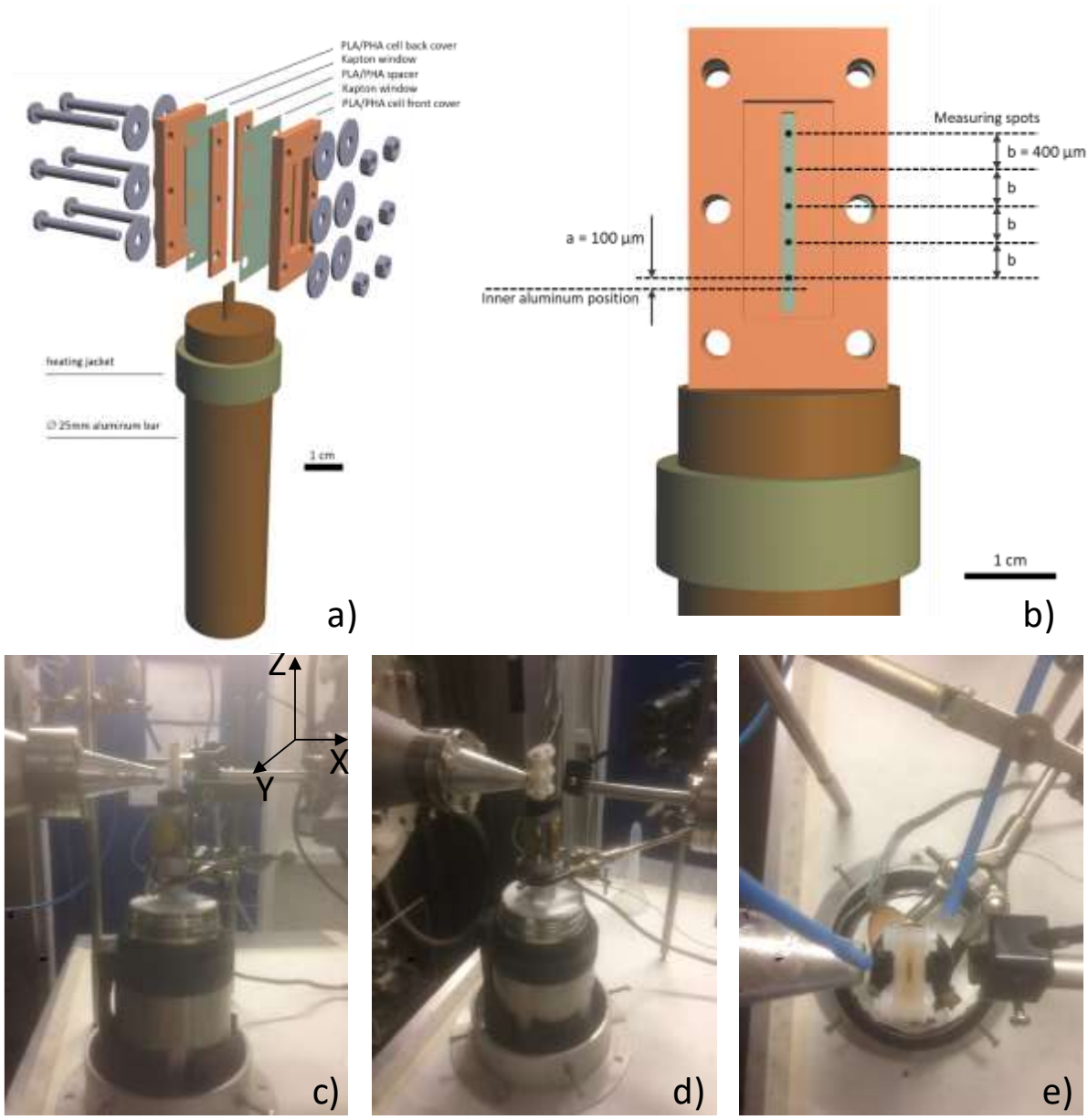

Figure S 3 – a) Freeze-casting setup used in synchrotron experiments. The bottom part of the aluminum bar (not shown) is kept in liquid nitrogen. The heating jacket is controlled by a dedicated PID and the temperature sensor (K thermocouple) is located at the top of the aluminum bar. b) Detail of the *in situ* freeze-casting cell used in synchrotron experiments. The cell is assembled from 3D printed PVA/PHA parts and kapton tape, assembled by 6 M6 nylon screws and knobs. The measuring position spots within the cell are indicated by black dots. c-e) Side, front and top views of the freeze-casting cell coupled to the ID02 beamline at ESRF synchrotron. The liquid nitrogen Dewar is located at the bottom of the cell is while the X-ray source is on the right-hand side. The blue pipes in (e) carry a constant air flux in the front and bottom of the cell to avoid condensation and crystallization of moisture.

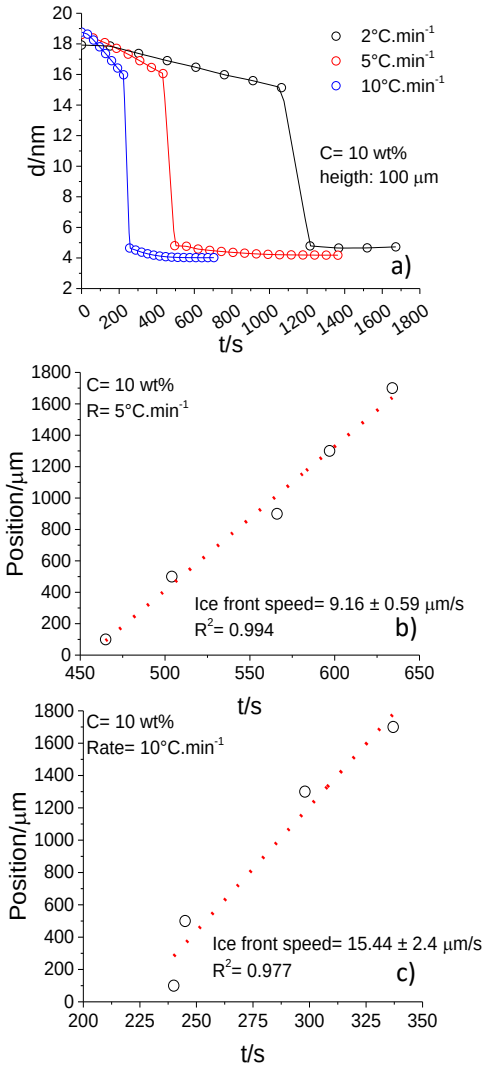

Figure S 4 – a) Raw data showing the evolution of lamellar *d*-spacing (extracted from *in situ* SAXS) with time measured for GC18:0 hydrogel (C= 10 wt%) at the position of 100 µm from the metal bar (Figure S 3b) for various freezing rates. The sudden drop in the *d*-spacing occurs during freezing and it is assumed to be the ice front. b-c) Evolution of the ice front at positions 100, 500, 900, 1300, 1700 µm from the metal bar (Figure S 3b) with time for the same GC18:0 hydrogel (C= 10 wt%) and two freezing rates (5°C.min^{-1} and 10°C.min^{-1}). Data are fitted linearly to estimate the ice front speed. By knowing the measuring position (Figure S 3b), the freezing rate and the ice front speed at a given rate, it is possible to precisely estimate the evolution of *d*-spacing with temperature at a given position and freezing rate. These data are shown in Figure 4c,d in the main manuscript. This calibration is necessary due to the large differences in terms of distance between position at 100 µm (where temperature is actually measured using a thermocouple) and 1700 µm.

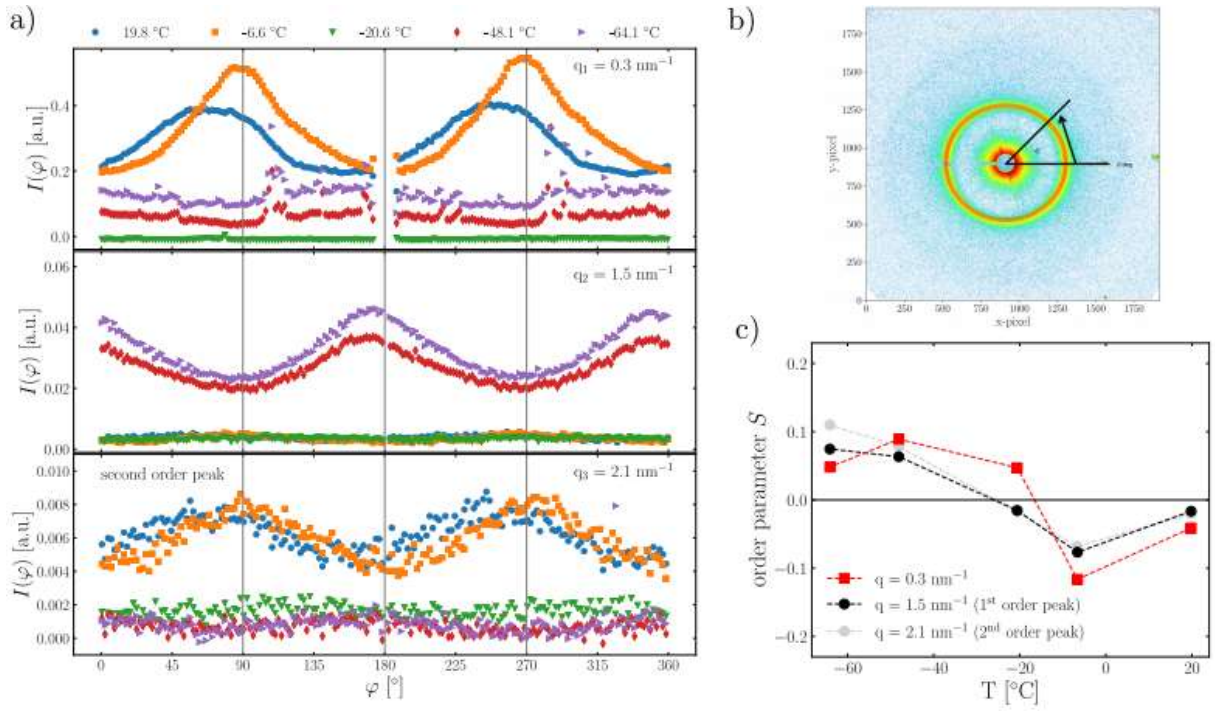

Figure S 5 - a) Azimuthal intensity distribution for the observed peaks at q = 0.3 nm^{-1} , q = 1.5 nm^{-1} and its second order peak at q = 2.1 nm^{-1}, b) 2D scattering pattern at T = -64.1°C with the indication of the φ-integration direction and c) obtained order parameter S as a function of temperature for the different peaks.

In Figure S 5a) the azimuthal intensity distribution on the observed peaks is shown as a function of azimuthal angle φ and temperature. The direction of azimuthal integration is depicted in Figure S 5b). For the higher temperatures one can also observe the second order peak at q_3=2.1 nm^{-1}. Hence, q_1 and q_3 have similar features i.e. orientation. Whereas q_2 appears from -20.6°C to the lowest measured temperature having a 90° shift in orientation. The peaks above -20.6°C completely disappeared. Having the data shown in Figure S 5a) one can easily calculate the orientation order parameter S for the different q values and temperatures according to

$$S_q = \langle P_2(cos\varphi)\rangle_q = \frac{3\langle cos^2\varphi\rangle_q - 1}{2}$$

with $\langle cos^2\varphi\rangle_q = \frac{\int_0^{\pi/2} I(q,\varphi)\, cos^2\varphi\, sin\varphi\, d\varphi}{\int_0^{\pi/2} I(q,\varphi)\, sin\varphi\, d\varphi}$. The obtained S is plotted in Figure S 5c as a function of temperature.

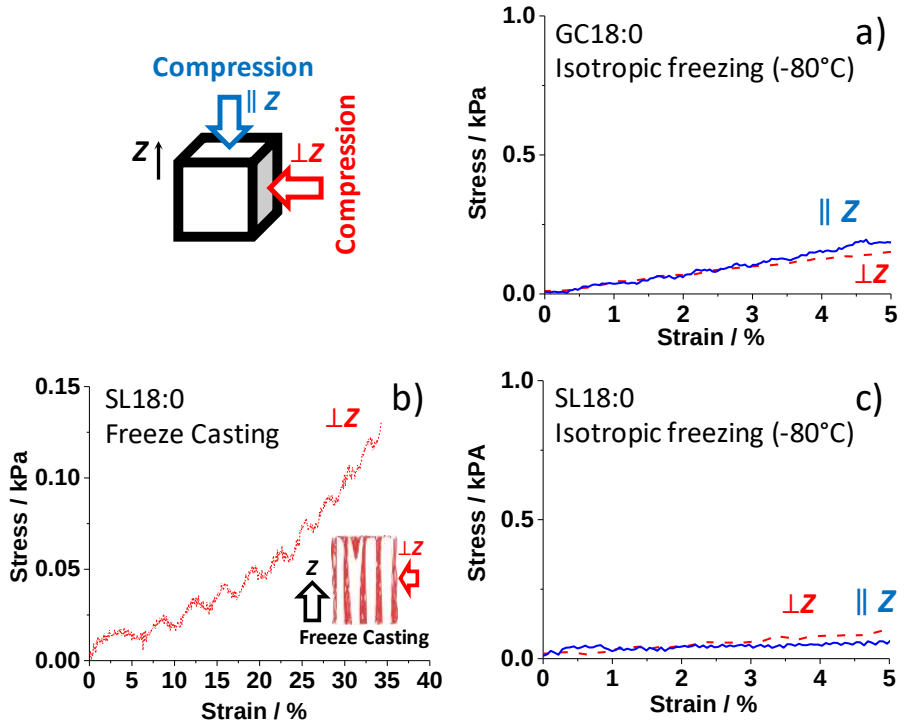

Figure S 6 – Stress–strain curves of SLC18:0 fibrillar and GC18:0 lamellar foams at 5 wt% measured on cubic samples (1 cm x 1 cm x 1 cm) by compression experiments along ∥*Z* (blue curves) and ⊥*Z* (red curves) according to the scheme. Experiments in a) and c) are recorded on samples, that are frozen in an isotropic environment at -80°C. Experiment in b) highlights a broad range of strain values (⊥*Z*) for the freeze-casting experiment shown in Figure 5b.

[1] A.-S. Cuvier, J. Berton, C. V Stevens, G. C. Fadda, F. Babonneau, I. N. a Van Bogaert, W. Soetaert, G. Pehau-Arnaudet and N. Baccile, *Soft Matter*, 2014, **10**, 3950–9

[2] N. Baccile, M. Selmane, P. Le Griel, S. Prévost, J. Perez, C. V. Stevens, E. Delbeke, S. Zibek, M. Guenther, W. Soetaert, I. N. A. Van Bogaert and S. Roelants, *Langmuir*, 2016, **32**, 6343–6359

[3] N. Baccile, A.-S. Cuvier, S. Prévost, C. V Stevens, E. Delbeke, J. Berton, W. Soetaert, I. N. A. Van Bogaert and S. Roelants, *Langmuir*, 2016, *32*, 10881–10894.

[4] G. Ben Messaoud, P. Le Griel, S. Prévost, D. H. Merino, W. Soetaert, S. L. K. W. Roelants, C. V. Stevens and N. Baccile, arXiv, 2019, 1907.02223

[5] G. Ben Messaoud, P. Le Griel, D. H. Merino, S. L. K. W. Roelants, C. V. Stevens and N. Baccile, *Chem. Mater.*, 2019, DOI: 10.1021/acs.chemmater.9b01230.

[6] S. Christoph, J. Kwiatoszynski, T. Coradin and F. M. Fernandes, *Macromol. Biosci.*, 2016, **16**, 182–187.

[7] U. G. K. Wegst, M. Schecter, A. E. Donius and P. M. Hunger, *Philos. Trans. R. Soc. A Math. Phys. Eng. Sci.*, 2010, **368**, 2099–2121.

[8] T. Narayanan, M. Sztucki, P. Van Vaerenbergh, J. Leonardon, J. Gorini, L. Claustre, F. Sever, J. Morse, and P.

Boesecke. A multipurpose instrument for time-resolved ultra-small-angle and coherent X-ray scattering, *J. Appl. Crystallogr*., 2018, **51** (Pt 6), 1511-1524

[9] C. A. Schneider, W. S. Rasband and K. W. Eliceiri, *Nat. Methods*, 2012, **9**, 671–675.